Electronic Supplementary Material (ESI) for Nanoscale.

Supporting Information

Formation of Bimetallic Dumbbell Shaped Particle with a Hollow Junction during Galvanic Replacement Reaction

Sravan Thota[a], Yadong Zhou[b], Shutang Chen[a], Shengli Zou[b], and Jing Zhao[a, c]

[a]Department of Chemistry, University of Connecticut, 55 North Eagleville Road, Storrs, Connecticut 06269-3060, United States

[b]Department of Chemistry, University of Central Florida, 4104 Libra Drive, Orlando, Florida 32816-2366, United States

[c]Institute of Materials Science, University of Connecticut, Storrs, Connecticut 06269-3136, United States.

* Address Correspondence to: jing.zhao@uconn.edu

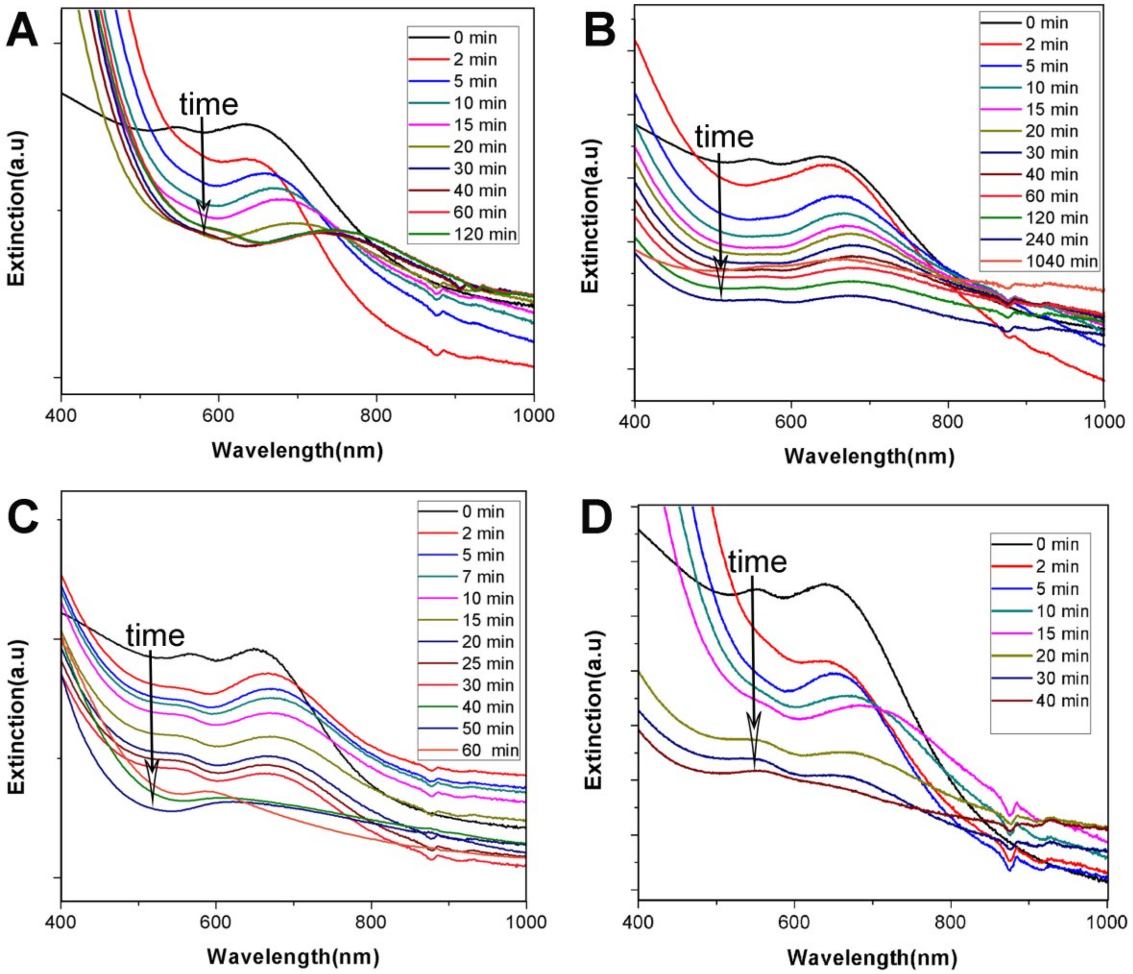

Figure S1. In situ UV-visible extinction spectra of AuCu alloy nanorods during galvanic replacement reaction with $HAuCl_4$ of different volumes (A) 0.65 mL, (B) 0.80 mL, (C) 1 mL and (D) 2 mL.

Table S1: Wavelength and intensity of major peak values during GRR, for four different concentrations of $HAuCl_4$

Time	**0.65 mL**		**0.80 mL**		**1 mL**		**2 mL**	
	λ_{max}	**I**	**λ_{max}**	**I**	**λ_{max}**	**I**	**λ_{max}**	**I**
0 min	644	0.85	644	0.87	652	0.96	644	0.86
2 min	649	0.73	651	0.84	667	0.86	650	0.72
5 min	666	0.67	665	0.74	673	0.79	656	0.69
10 min	679	0.59	667	0.69	679	0.69	677	0.65
15 min	690	0.53	674	0.65	682	0.59	700	0.55
20 min	700	0.46	678	0.63	677	0.50	671	0.51
30 min	738	0.43	684	0.59	673	0.44	659	0.45
40 min	738	0.43	686	0.56	611	0.34	572	0.42
60 min	763	0.44	686	0.51	605	0.35		
120 min	763	0.44	686	0.48	593	0.35		

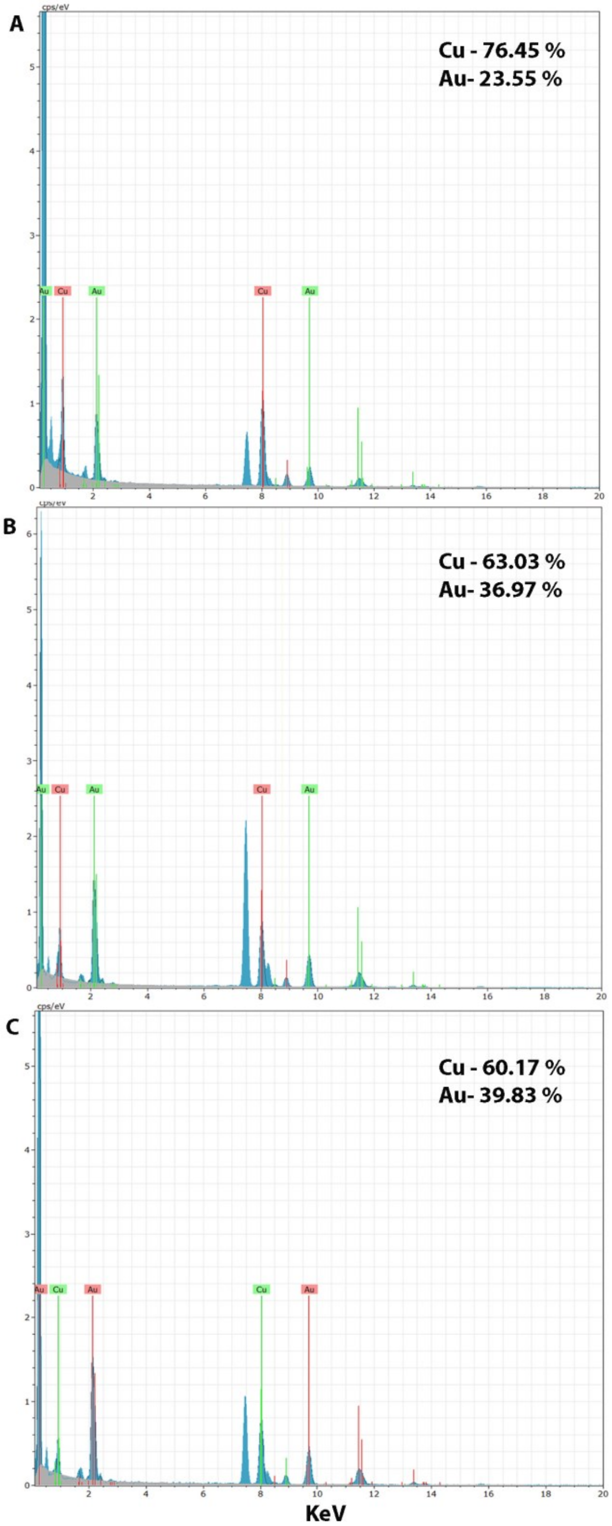

Figure S2. EDS of initial $AuCu_3$ rods (A) and samples separated after 30 min (B), and 1 hr (C) after adding $HAuCl_4$.

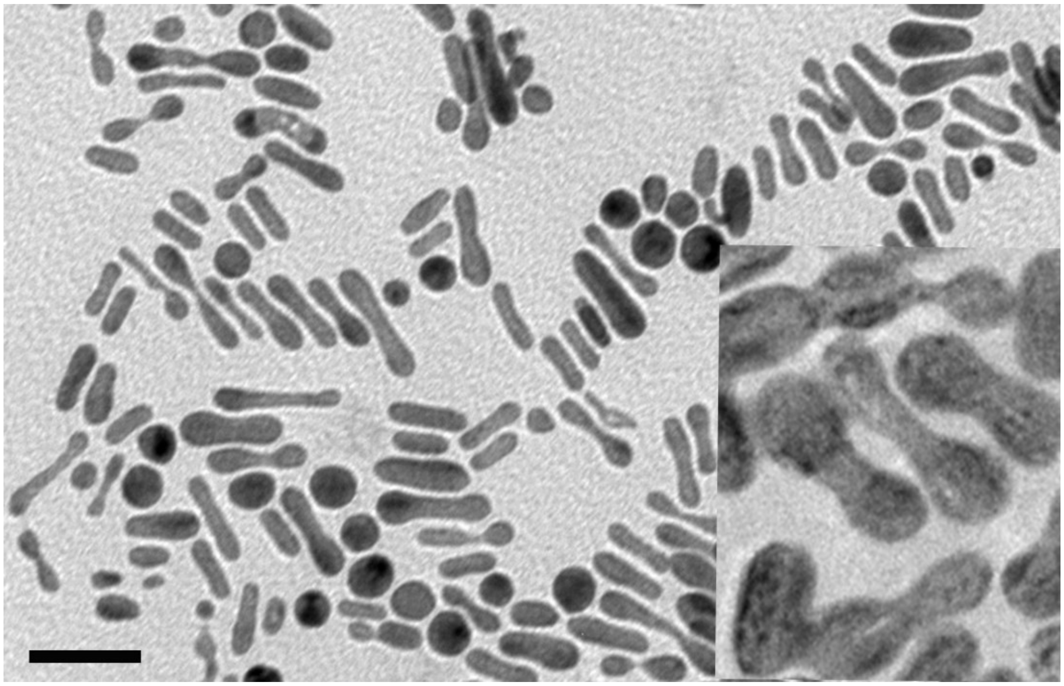

Figure S3. TEM image of the sample separated at 45 min. Inset indicates peanut shaped particles with different junction diameters, indicating the reaction kinetics of individual particles is different. Scale bar=50 nm.

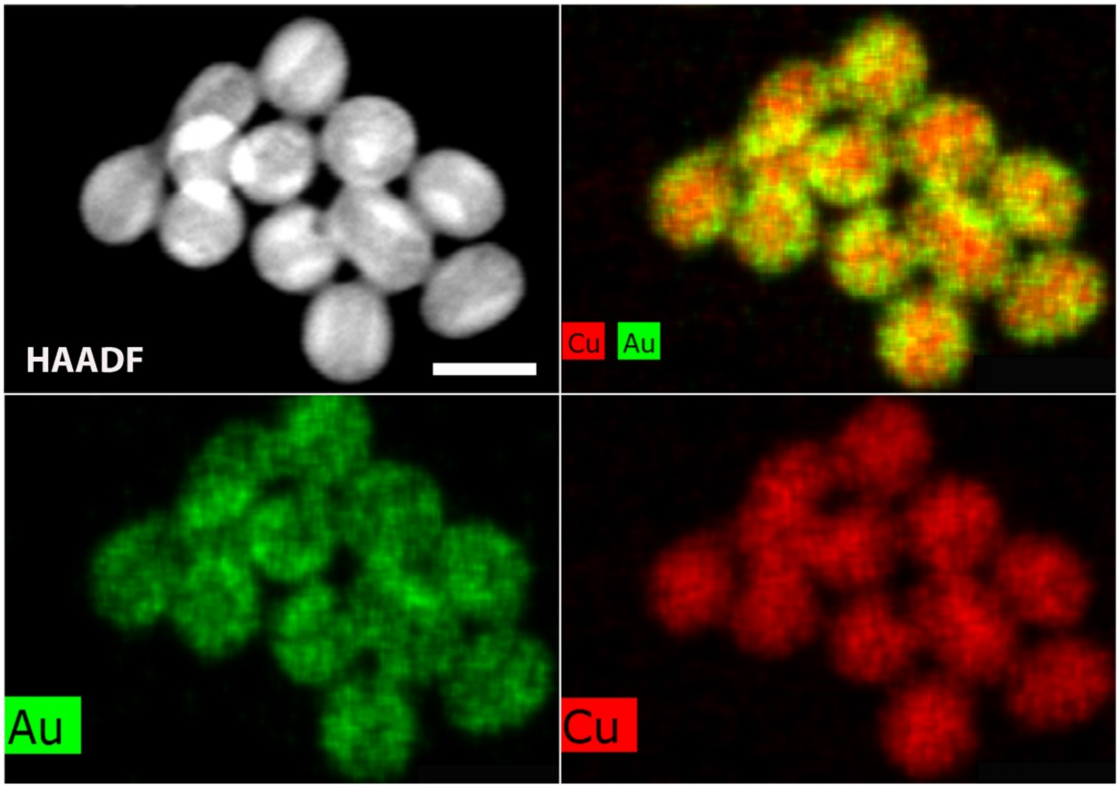

Figure S4. EDX elemental mapping of the sample obtained after 1 hr of reaction. The overlaid image clearly indicates the Au@AuCu structure similar to the ends of the intermediate separated at 30 min.

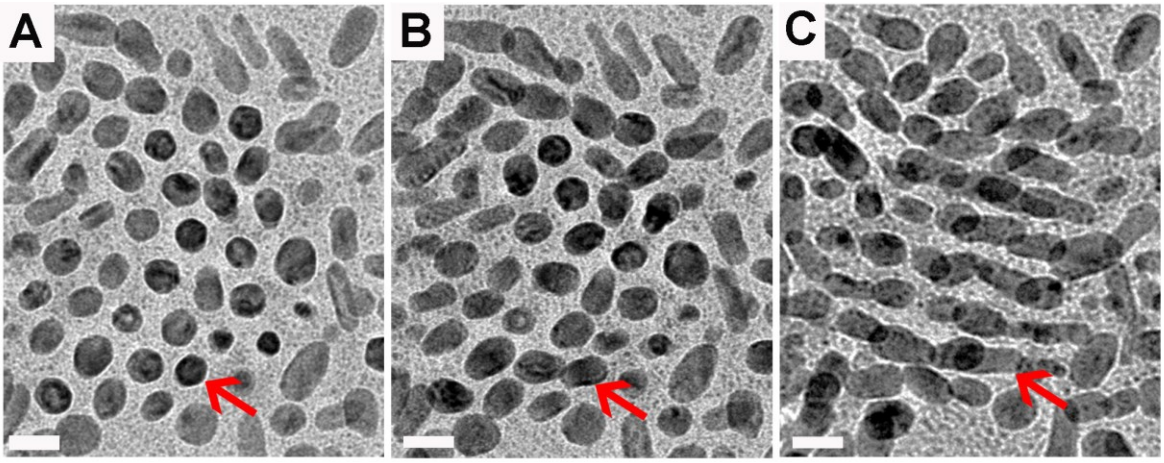

Figure S5. $AuCu_3$ nanorod tip analysis. (A-C) TEM images of a standing $AuCu_3$ alloy nanorods viewed by rotating the stage to different angles, with red arrow pointing to one particular rod.

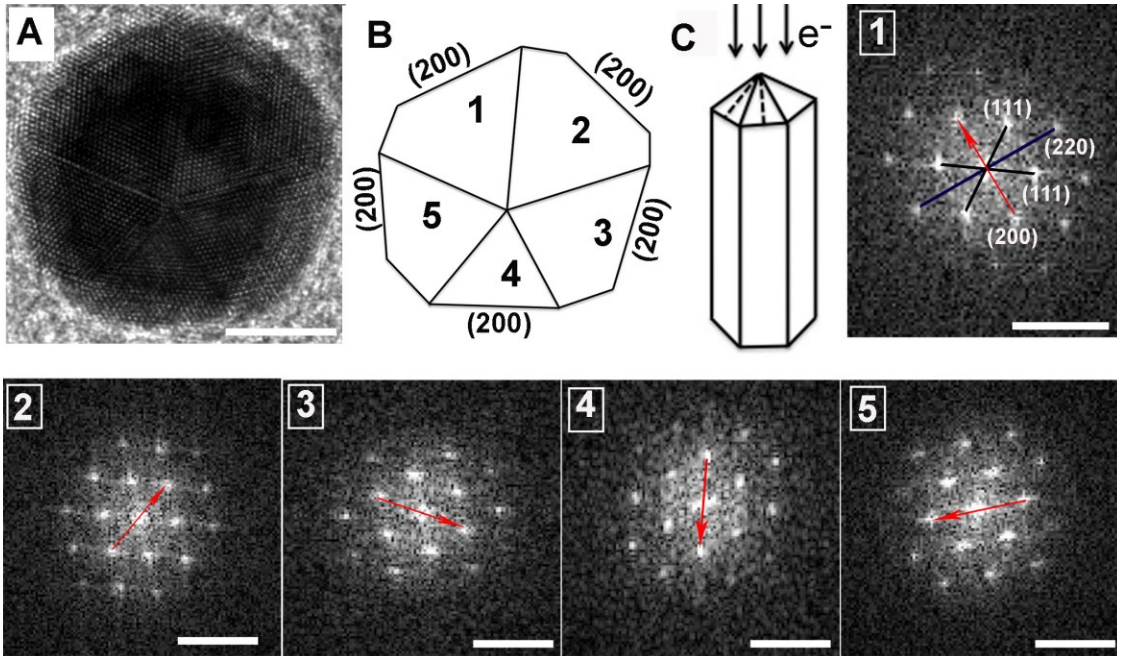

Figure S6. $AuCu_3$ nanorod tip analysis. (A) HRTEM image of a standing $AuCu_3$ alloy nanorod. (B) Representation of (A), showing penta twinned structure with major (200) facets. (C) Representation of a standing nanorod and electron beam direction. (1-5) Corresponding FFT patterns of each twin plane represented in (B). Red arrow indicates (200) direction in each plane. The scale bar for HRTEM= 5 nm and FFT patterns= 10.1 nm

Table S2. Peak wavelengths of single particle scattering spectra from figure 6

Time (min)	**Figure 6A- λ_{max}**	**Figure 6B- λ_{max}**	**Figure 6C- λ_{max}**
0 min	634	634	672
2 min	637	636	677
5 min	639	641	681
7 min	653	669	692
10 min	664	676	694
15 min	672	679	695
20 min	681	681	695
30 min	706	689	700
40 min	643	613	632
60 min	628	613	609
120 min	628	620	601

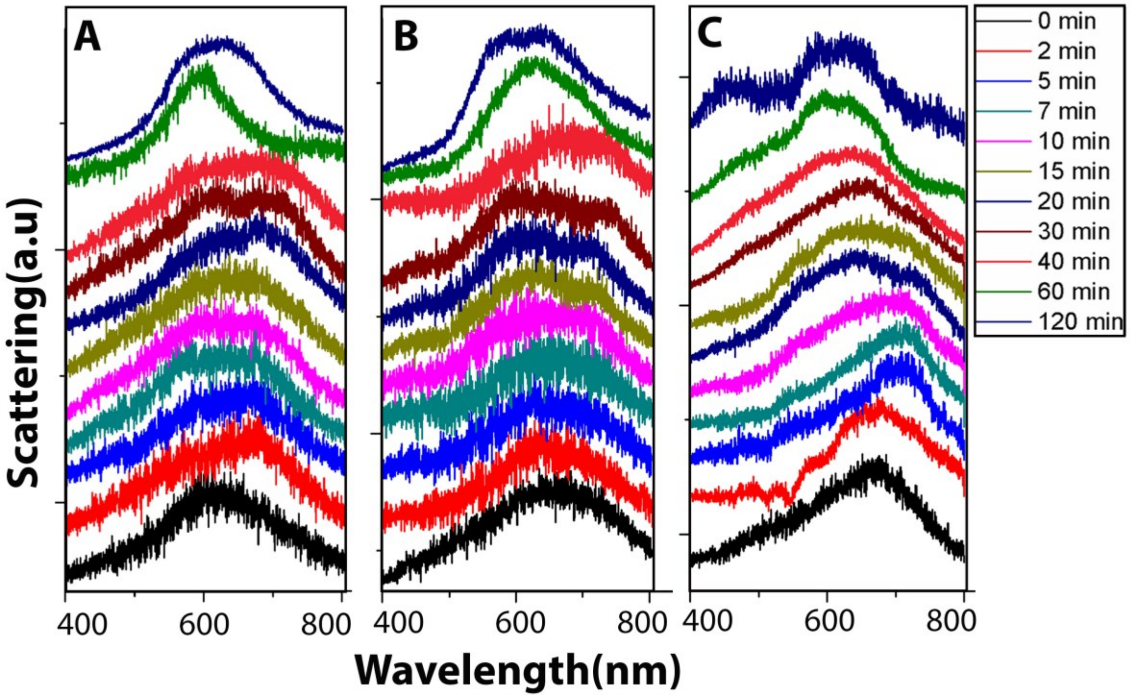

Figure S7. In situ dark field scattering spectra of Au-Cu alloy nanorods during galvanic replacement with $HAuCl_4$. A, B, C are traces of three individual nanorods during galvanic exchange, showing initial red shift with a shoulder around 600 nm. The shoulder grows stronger at later stages.

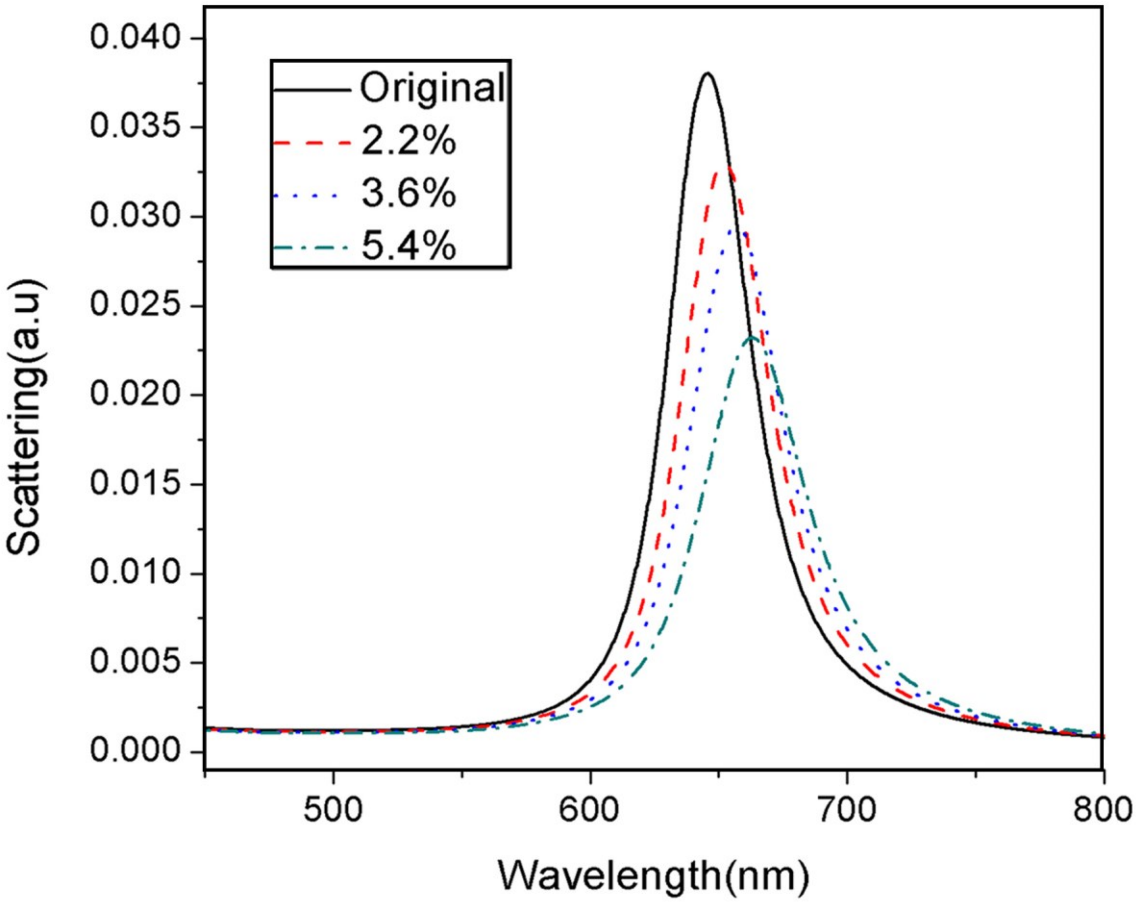

Figure S8. Calculated scattering spectra of the $AuCu_3$ nanorod (black) and after different extents of galvanic replacement on the surface of the nanorod, Red: 2.2%, blue: 3.6%, and Cyan: 5.4%. Galvanic replacement on the surface at the initial stages only causes red shift in the longitudinal mode of the nanorod.

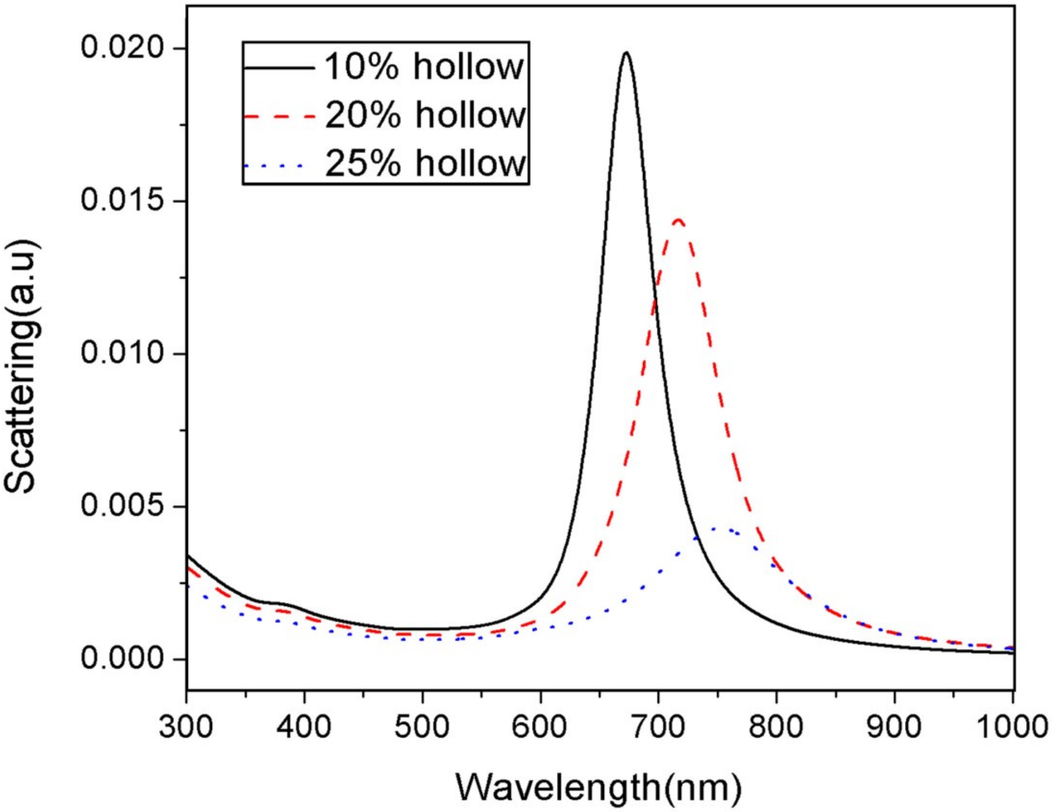

Figure S9. Calculated scattering spectra of the $AuCu_3$ nanorod with different %volumes of hollowness at random locations, black: 10%, red: 20%, and blue: 25%. Hollowing at random locations other than center of the nanorod only cause red shift in the longitudinal mode, but doesn't cause peak splitting. This indicates the experimentally observed peak splitting in in situ experiments was due to creation of hollow region exactly at the center of the nanorod resulting from tip preferential Cu diffusion.

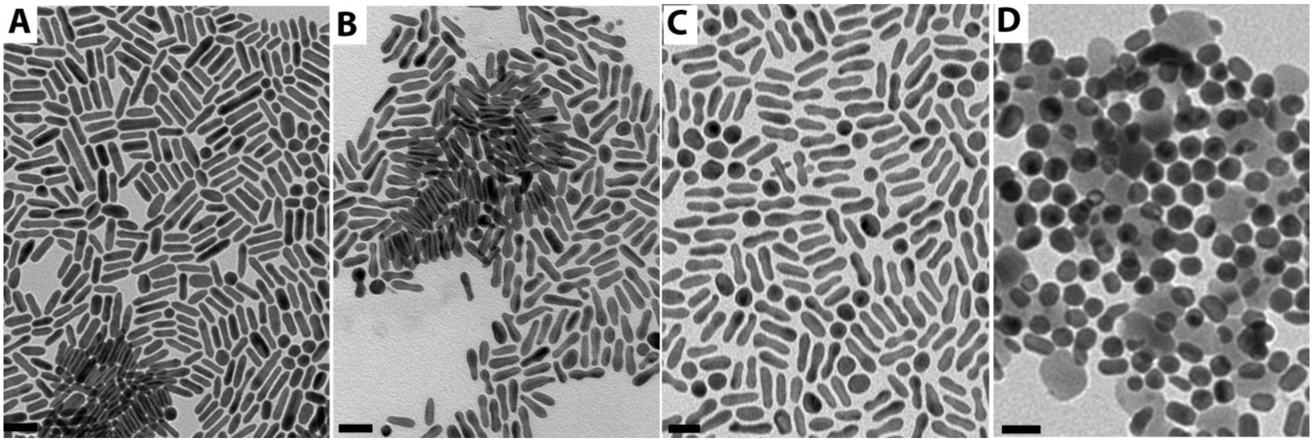

Figure S10. TEM images of the samples, (A) Initial $AuCu_3$ nanorods, (B), (C) and (D) are samples obtained after 10 min, 20 min and 45 min of galvanic replacement reaction performed on Ni grid. The scale bar= 50 nm.

To perform the experiments, $AuCu_3$ nanorods were deposited on carbon supported TEM grid and dried. 1 mL $HAuCl_4$ was added to the samples and reacted with the nanorods for desired time. The $HAuCl_4$ was then removed using a KimWipe. The sample was allowed to dry for TEM measurements. The morphology of the intermediates and final products obtained here is similar to that of the samples acquired in solution phase GRR. The results show that the GRR reaction pathway on substrate is similar to that of solution phase. And it also showed that dissolving Au precursor in water has no effect on reaction mechanism.

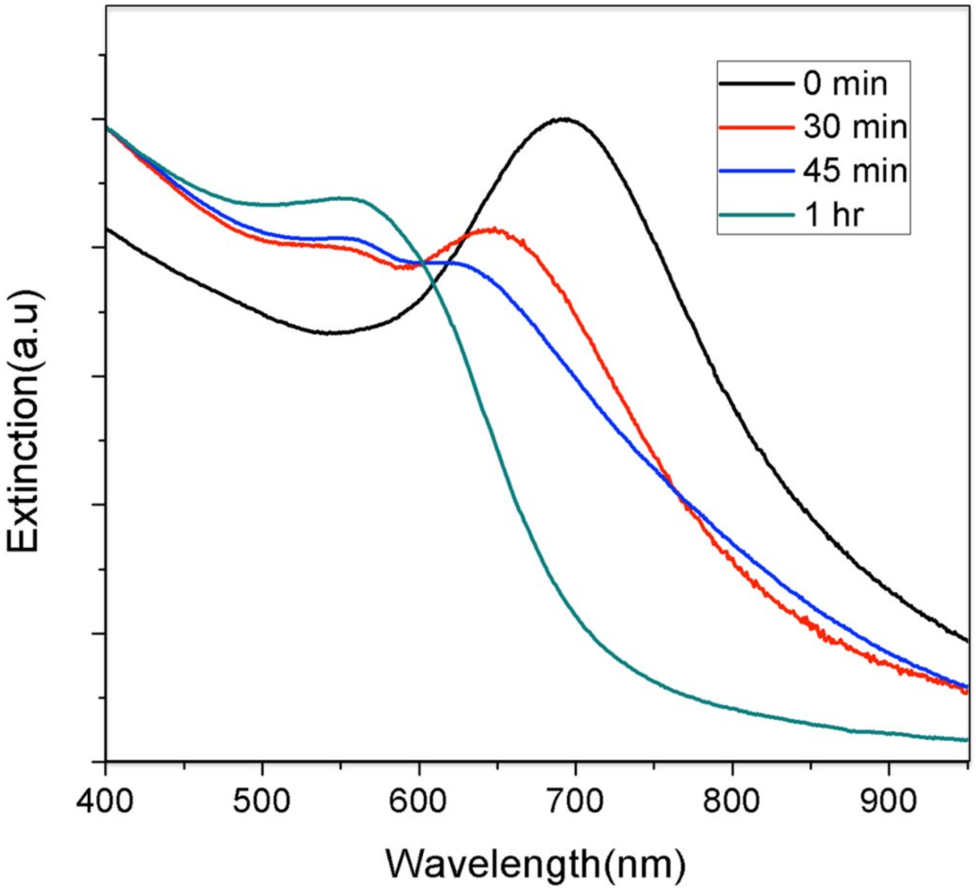

Figure S11. Ensemble extinction spectra of initial $AuCu_3$ nanorods (black) and samples separated at 30 min (red), 45 min (blue) and 1 hr (scion). The blue shift followed by increase in peak intensity at 570 nm indicates formation of Au Cu alloy nanoparticles.